JOC The Journal of Organic Chemistry

Article

pubs.acs.org/joc

Strongly Chemiluminescent Acridinium Esters under Neutral Conditions: Synthesis, Properties, Determination, and Theoretical Study

Manabu Nakazono,*[,†] Yuji Oshikawa,[†] Mizuho Nakamura,[‡] Hidehiro Kubota,[§] and Shinkoh Nanbu[‡]

[†]Graduate School of Pharmaceutical Sciences, Kyushu University, 3-1-1 Maidashi, Higashi-ku, Fukuoka 812-8582, Japan

[‡]Faculty of Science and Technology, Sophia University, 7-1 Kioi-Cho, Chiyoda-ku, Tokyo 102-8554, Japan

[§]ATTO Corporation, 3-2-2 Motoasakusa, Taito-ku, Tokyo 111-0041, Japan

Supporting Information

ABSTRACT: Various novel acridinium ester derivatives having phenyl and biphenyl moieties were synthesized, and their optimal chemiluminescence conditions were investigated. Several strongly chemiluminescent acridinium esters under neutral conditions were found, and then these derivatives were used to detect hydrogen peroxide and glucose. Acridinium esters having strong electron-withdrawing groups such as cyano, methoxycarbonyl, and nitro at the 4-position of the phenyl moiety in phenyl 10-methyl-10λ^4-acridine-9-carboxylate trifluoromethanesulfonate salt showed strong chemiluminescence intensities. The chemiluminescence intensity of 3,4-dicyanophenyl 10-methyl-10λ^4-acridine-9-carboxylate trifluoromethanesulfonate salt was approximately 100 times stronger than that of phenyl 10-methyl-10λ^4-acridine-9-carboxylate trifluoromethanesulfonate salt at pH 7. The linear calibration ranges of hydrogen peroxide and glucose were 0.05−10 mM and 10−2000 μM using 3,4-(dimethoxycarbonyl)phenyl 10-methyl-10λ^4-acridine-9-carboxylate trifluoromethanesulfonate salt at pH 7 and pH 7.5, respectively. The proposed chemiluminescence reaction mechanism of acridinium ester via a dioxetanone structure was evaluated via quantum chemical calculation on density functional theory. The proposed mechanism was composed of the nucleophilic addition reaction of hydroperoxide anion, dioxetanone ring formation, and nonadiabatic transition due to spin−orbit coupling around the transition state (TS) to the triplet state (T_1) following the decomposition pathway. The TS which appeared in the thermal decomposition would be a rate-determining step for all three processes.

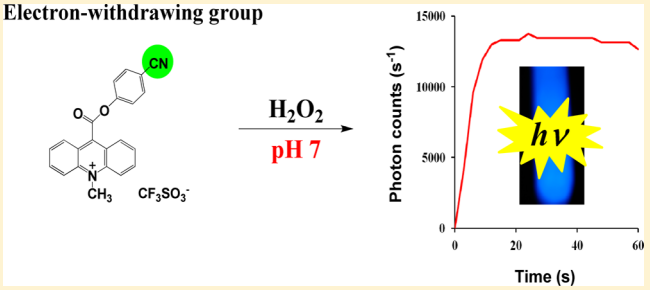

INTRODUCTION

Chemiluminescence (CL) assays have been utilized for determining various kinds of compounds qualitatively and quantitatively.[1−11] CL compounds have been developed as useful luminescent reagents. In particular, luminol (3-aminophthalhydrazide) derivatives,[12−21] acridinium ester derivatives,[22−30] and dioxetane derivatives[31−37] are essential compounds in highly sensitive CL assays. Recently, luminol was applied to CL imaging in vivo by CL resonance energy transfer (CRET).[38] Acridinium ester derivatives have been frequently selected for enzyme immunoassays.[39−41] Intramolecular chemically initiated electron exchange luminescence mechanism and CRET were applied to acridinium-substituted 1,2-dioxetanes.[42] CL sensing of fluoride ions using a self-immolation mechanism was developed based on dioxetane CL.[43] The CL properties and mechanism of 2-coumaranones were clarified by experimental and theoretical study.[44]

Acridinium esters react with hydrogen peroxide to produce fluorescent 10-methyl-9-acridone via a dioxetanone structure (Scheme 1).[45,46a] Acridinium ester derivatives have relatively strong CL intensity among CL compounds, and various derivatives can be synthesized in a facile manner. 10-Carboxymethylacridinium derivatives were synthesized when a methyl group (an electron-donating group) was introduced at the 2- and 6-positions of the phenyl moiety, resulting in strong CL intensity.[23] 9-Acridinecarboxylic esters of hydroxamic and sulfohydroxamic acids had strong CL intensity at picomolar levels.[25] Acridinium dimethylphenyl esters containing *N*-sulfopropyl groups in the acridinium ring were highly sensitive CL compounds.[39b] 2′,6′-Dimethyl-4′-(*N*-succinimidyloxycarbonyl)phenyl-10-methyl-acridinium-9-carboxylate-1-propanesulfonate inner salt was used for capillary CL determination of sympathomimetic drugs.[47] These CL compounds were dissolved in acetonitrile or dimethylformamide, and the CL was measured in sodium hydroxide and hydrogen peroxide solution. In general, most CL compounds require strong alkaline conditions and the CL signals are short lasting. A little was studied about acridinium esters having novel CL properties under neutral conditions. Di-*o*-bromophenyl acridinium ester

Received: November 30, 2016
Published: February 7, 2017

DOI: 10.1021/acs.joc.6b02748
J. Org. Chem. 2017, 82, 2450−2461

Scheme 1. Chemiluminescence Mechanism of Acridinium Esters

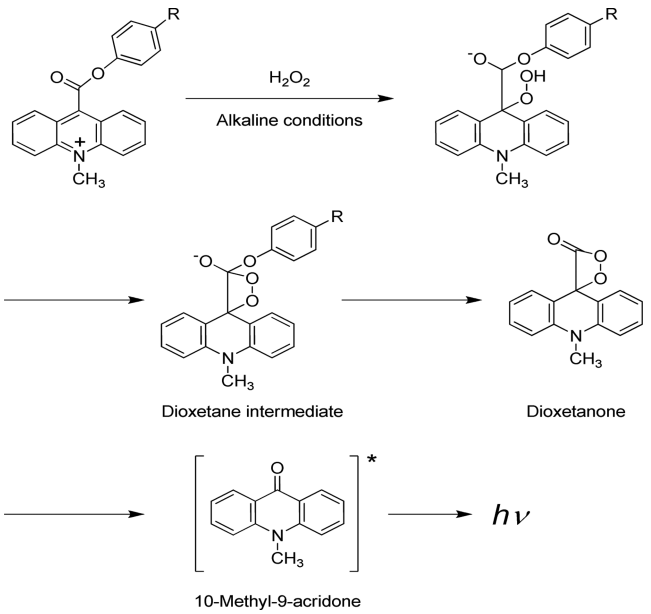

generated CL signal under neutral conditions.[48,49] If compounds exhibiting strong CL under neutral conditions could be identified, it would be possible to develop novel and useful CL assays. For example, in the CL measurement of an enzyme activity producing hydrogen peroxide under neutral conditions, the enzyme activity could be measured without the addition of alkali. Therefore, a method is needed to synthesize acridinium esters that can readily react with hydrogen peroxide under neutral conditions. In a previous study, the introduction of electron-withdrawing groups such as bromide to the 4-position of the phenyl moiety in phenyl 10-methyl-10λ^4-acridine-9-carboxylate trifluoromethanesulfonate salt was shown to increase the CL intensity of acridinium esters.[46a] Electron-withdrawing groups could polarize the electron density toward the phenyl ring and thereby reduce the electron density at the C9 position of the acridine moiety. Hydroperoxide anion (HOO^-) reacts with the C9 position in a facile manner, and light is produced.[46a] First, therefore, we decided to focus on cyano, trifluoromethyl, methoxycarbonyl, and nitro groups. We thus considered that the detailed effects of electron-donating groups and electron-withdrawing groups on the 4-position of the phenyl moiety in phenyl 10-methyl-10λ^4-acridine-9-carboxylate trifluoromethanesulfonate salt should also be evaluated. In a related experiment, we investigated the increase of CL intensity by the increase of acridinium moieties. Second, the crystal structure of [1,1′-biphenyl]-4-yl 10-methyl-10λ^4-acridine-9-carboxylate trifluoromethanesulfonate salt was previously determined, and the two phenyl rings of the biphenyl moiety were oriented at a dihedral angle of 42.9°.[50] We predicted that the twist structure of the biphenyl moiety would cause rapid cleavage of the biphenoxy moiety in the dioxetane intermediate and thereby increase the production of 10-methyl-9-acridone and the level of CL intensity. Thus, various derivatives of [1,1′-biphenyl]-4-yl 10-methyl-10λ^4-acridine-9-carboxylate trifluoromethanesulfonate salt were synthesized.

Useful CL methods for determining various analytes are developed by measurement of enzymatically generated hydrogen peroxide. For example, glucose reacts with glucose oxidase (EC1.1.3.4) in the presence of oxygen, and hydrogen peroxide is generated. The quantification of glucose can be achieved by the reaction of hydrogen peroxide and CL compound. In this study, various novel acridinium ester derivatives were designed and synthesized, and their CL was measured. Finally, novel acridinium esters, which appear to have strong CL intensity under neutral conditions, were developed and utilized for the CL determination of hydrogen peroxide and glucose. Furthermore, a theoretical study was performed to clarify the charge distributions of C9 and N10 positions of acridine moiety and energy diagram on the proposed CL mechanism by ab initio chemical calculations.

RESULTS AND DISCUSSION

Synthesis of Compounds 1−26. Acridine-9-carbonyl chloride and biphenols were prepared by previously described methods.[51,52] The esterification reaction of acridine-9-carbonyl chloride and phenols proceeded promisingly in the presence of triethylamine, 4-dimethylaminopyridine, and tetrahydrofuran. Methyl trifluoromethanesulfonate was used for the N-methylation of acridine moieties in dichloromethane (Table 1). As shown in Table 2, 4-iodophenol was transformed by arylboronic acids through Suzuki−Miyaura coupling, and compounds **18−20** were synthesized in a facile manner. In the synthesis of compound **26**, 1,1′:4′,1″-terphenyl-4-ol was prepared with 4-bromo-4′-hydroxyphenyl and phenylboronic acid in the presence of tetrakis(triphenylphosphine)palladium, potassium carbonate, and dimethoxyethane.[53] In the purification of compounds **1−26** by column chromatography, the crude products were excluded by chloroform−methanol solution (v/v, 20/1), and compounds **1−26** were eluted by using chloroform−methanol solution (v/v, 5/1, 4/1 or 2/1).

Chemiluminescence Properties of Compounds 1−26. Compounds **3**, **4**, and **9−13** had particularly strong CL intensities at pH 7. The CL of compounds **3** and **10−13** was long-lasting.

In compound **3**, the time required to the maximum photon count was 15 s after the addition of hydrogen peroxide (Figure 1A). In contrast, the CL intensities of compound **1** and luminol were very weak at pH 7. Compared to the CL curves of compounds **3**, **9**, **12**, and **13**, increasing the number of electron-withdrawing groups on the phenyl moiety caused the increase of CL intensity. Compound **3** produced CL in phosphate buffer at pH 7, and blue light emission was observed (Figure 1B). The effect of pH on the CL development of compounds **1−17** is shown in Figure 2. Novel acridinium esters that can produce strong CL were found under neutral conditions (pH 7 and pH 8). Most of compounds **1−17** had maximum CL intensities at pH 8. However, the CL intensities of compounds **1** and **5** increased under alkaline conditions (pH 9 and pH 10). In compounds **2−17**, the CL intensities appeared to be greater than that of compound **1** at pH 7 (Figure 3). The CL intensity of compound **12** was approximately 100 times stronger than that of compound **1** at pH 7. The introduction of strong electron-withdrawing groups such as cyano, methoxycarbonyl, and nitro at the 4-position of the phenyl moiety increased the CL intensity and that of electron-donating groups such as methyl and methoxy decreased the CL intensity. Quantum yields of acridinium esters are correlated with the pK_a of the leaving group.[54] The pK_a values of phenols having electron-withdrawing groups at the 4-position of the phenol moiety are 7.1−8.5.[55] When electron-withdrawing groups to the 4-position of the phenyl moiety are introduced, the pK_a of the leaving

DOI: 10.1021/acs.joc.6b02748
J. Org. Chem. 2017, 82, 2450−2461

Table 1. Synthesis and Chemical Structure of Compounds 1−17

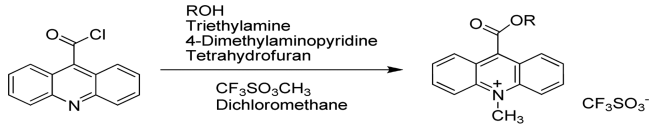

Compounds **1**–**17**

Compound	R	Yield (%)	Compound	R	Yield (%)
1		13	**10**	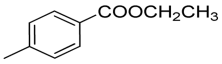	4
2	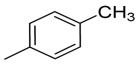	14	**11**	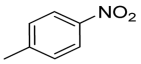	46
3	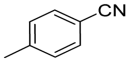	23	**12**	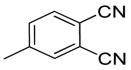	12
4	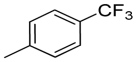	13	**13**	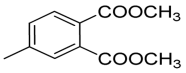	13
5	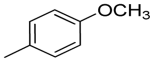	25	**14**	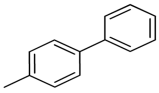	23
6	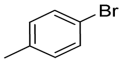	63	**15**	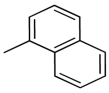	50
7	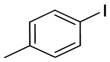	26	**16**	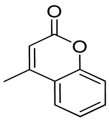	4
8	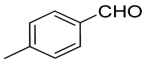	57	**17**	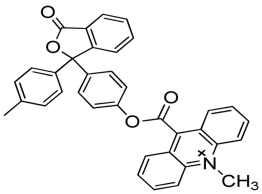	21
9	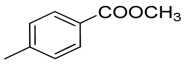	30			

group decreases.[55] On the basis of the CL mechanism of acridinium ester (Scheme 1), the phenyl moiety of compounds **3**, **4**, and **8**−**13** probably leaves and 10-methyl-9-acridone is produced. In 100 mM phosphate buffer (pH 7), the relative CL intensities of compounds **1**, **3**, **4**, **8**, **9**, **10**, **11**, and **13** were similar to those in 100 mM Tris-HCl (Figure S1 in Supporting Information). Acridinium esters exist in equilibrium with their corresponding pseudobases (Figure 4) in aqueous solution.[39a] The pseudobase is a nonchemiluminescent compound. When the pseudobase formation is suppressed, the CL intensity may increase. The absorption spectra of compounds **1** and **3** were measured in Tris-HCl solution (pH 7 and pH 8). The absorption maxima of pseudobases were observed at approximately 280 nm,[56] and the apparent difference of these spectra was not observed (Figure S4 in Supporting Information). In compound **3**, the pseudobase formation is not suppressed under neutral conditions. Thus, pseudobase formation could not be a crucial factor in the strong CL intensity of compound **3** under neutral conditions. In comparing the CL intensities of compound **1** and compound **14**, it appeared that the twist structure of the biphenyl group was not the cause of the increase of CL intensity. The stabilities of compounds **1**, **3**, **4**, and **10**−**13** (10 nM) in dimethyl sulfoxide (25 °C, 3 h) were approximately 80%, 90%, 90%, 80%, 85%, 70%, and 94%. Most of compounds **18**−**26** had maximum CL intensities at pH 9 (Figure S2 in Supporting Information). The introduction of various functional groups to the biphenyl moiety (Table 2) appeared to be reasonable for the change of CL intensity. Specifically, the introduction of a methoxycarbonyl (compound **22**) and a nitro group (compound **25**) at the 4-position of the biphenyl moiety caused an increase of CL intensity (Figure S3 in Supporting Information). The CL intensity of compound **25** at pH 8 was approximately 5 times stronger than that of compound **14**. Unfortunately, the CL intensity of compound **26** did not increase (Table S1 in Supporting Information). Taken together, these results demonstrate that the introduction of electron-withdrawing groups to the 4-position of the phenyl and biphenyl moieties is crucial for increasing the CL intensity of acridinium esters.

DOI: 10.1021/acs.joc.6b02748
J. Org. Chem. 2017, 82, 2450−2461

Table 2. Synthesis and Chemical Structure of Compounds 18−26

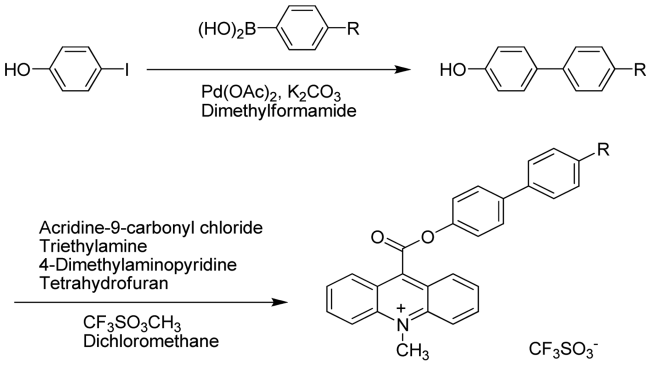

Compounds **18**–**26**

compound	R	yield (%)
18	CH_3	33
19	CH_2CH_3	5
20	OCH_3	12
21	Br	29
22	$COOCH_3$	11
23	$COOCH_2CH_3$	20
24	COOBn	9
25	NO_2	45
26	Ph	6

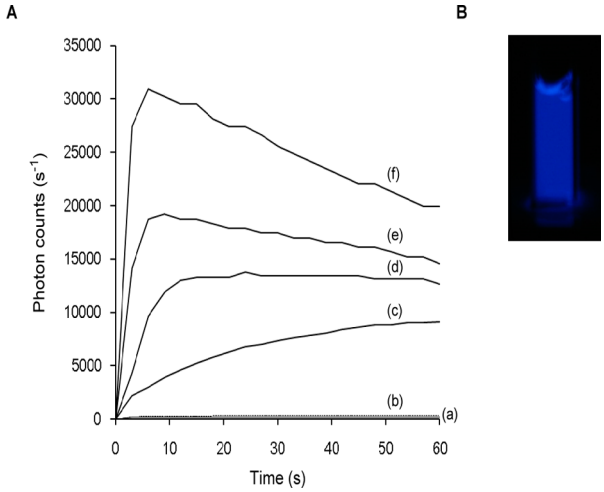

Figure 1. (A) Time-course of the chemiluminescence development of compounds **1**, **3**, **9**, **12**, **13**, and luminol in 100 mM Tris-HCl buffer at pH 7: (a) luminol; (b) compound **1**; (c) compound **9**; (d) compound **3**; (e) compound **13**; (f) compound **12**. The concentration of compounds **1**, **3**, **9**, **12**, **13**, and luminol was 10 nM. The concentration of hydrogen peroxide was 5 mM. (B) Chemiluminescence of compound **3** (100 μM) in 100 mM phosphate buffer at pH 7.

Standard Curves for Hydrogen Peroxide at pH 7 and pH 8 Using Compounds 3, 4, and 13. Compounds **3**, **4**, and **13** having high chemical stability were used for determination of hydrogen peroxide. The CL intensities of compounds **1**−**17** increased with the increase of hydrogen peroxide concentration (5−100 mM) at pH 7. Standard curves for hydrogen peroxide at pH 7 and pH 8 using compounds **3**, **4**, and **13** are shown in Figure 5. The linear calibration ranges of hydrogen peroxide were 0.05−25 mM (regression equation: $y = 121812x + 68861$, $R = 0.997$) at pH 7 and 0.05−5 mM (regression equation: $y = 613613x + 126736$, $R = 0.996$) at pH 8 using compound **3**. The relative standard deviation was mostly within 4.8% ($n = 3$). The detection limits ($S/N = 2$) of hydrogen peroxide were 50 μM at pH 7 and pH 8, respectively. The linear calibration ranges of hydrogen peroxide were 0.1−40 mM (regression equation: $y = 33036x + 52387$, $R = 0.997$) at pH 7 and 0.05−5 mM (regression equation: $y = 340474x + 41759$, $R = 0.999$) at pH 8 using compound **4**. The relative standard deviation was mostly within 5.8% ($n = 3$). The detection limits ($S/N = 2$) of hydrogen peroxide were 100 μM at pH 7 and 50 μM at pH 8. The linear calibration ranges of hydrogen peroxide were 0.05−10 mM (regression equation: $188851x + 12236$, $R = 0.999$) at pH 7 and 0.025−1 mM (regression equation: $y = 1120300x + 21398$, $R = 0.999$) at pH 8 using compound **13**, respectively. The relative standard deviation was mostly within 4.3% ($n = 3$). The detection limits ($S/N = 2$) of hydrogen peroxide were 50 μM at pH 7 and 25 μM at pH 8, respectively. A long-range of detectability and satisfactory reproducibility for the detection of hydrogen peroxide were obtained at pH 7 and pH 8. Similar standard curves were obtained at pH 7 and pH 8 in 100 mM phosphate buffer (Figure S5 in Supporting Information). In particular, the linear calibration ranges of hydrogen peroxide were 0.01−5 mM ($R = 0.993$) at pH 7 and 5−1000 μM ($R = 0.999$) at pH 8 using compound **13**, respectively. The relative standard deviation was mostly within 5.4% ($n = 3$). The detection limits ($S/N = 2$) of hydrogen peroxide were 10 μM at pH 7 and 5 μM pH 8, respectively. Compounds **3**, **4**, and **13** were thus shown to be suitable for the CL determination of hydrogen peroxide under neutral conditions.

Standard Curves for Glucose Using Compound 13. Compound **13** was very stable, used for the determination of hydrogen peroxide and applied for highly sensitive detection of glucose (Scheme 2). The linear calibration range of glucose was 10−2000 μM (regression equation: $y = 175.93x + 8131.4$, $R = 0.999$) at pH 7.5 using compound **13** (Figure 6). The relative standard deviation was mostly within 4.1% ($n = 3$). The detection limit (defined as the mean value of blank + 5σ) of glucose was 5 μM. This CL method of glucose showed similar sensitivity and linearity compared to the previous CL methods such as 1-ethyl-3-methylimidazolium ethylsulfate/Cu^{2+}−luminol−glucose oxidase, luminol−H_2O_2−horseradish peroxide−glucose oxidase, and the Cu^{II}-catalyzed CL of lucigenin using synthetic imidazolium-based ionic liquid derivatives.[57−59] Thus, this CL method can detect glucose at relatively high sensitivity without the addition of alkali and catalyst.

Theoretical Analysis. The potential energy of the S_0 state for compound **1** has been theoretically explored in detail by Błażejowski et al.;[56,60] the energy diagrams on the electronic ground state (S_0) have been determined for 10-methyl-9-(phenoxycarbonyl)acridium cations substituted with various alkyl groups in the phenyl fragment. However, the final products were assumed to be the electronic ground states for *N*-methylacridone (NMA) in their work. To make the acridone molecule emit a photon, the electronically excited states of NMA have to be found at the end of this reaction in the proposed CL reaction mechanism by McCapra and Nelson.[45,46a] In the present work, the energetics were mainly explored by the density functional theory (DFT)-based B3-LYP functional at the correlation-consistent polarized-valence double-ζ (cc-pVDZ) basis function[61] for (i) the thermally accessible dioxetanone to reach an electronic excited state of acridone molecule in S_0, (ii) nonadiabatic transition through spin−orbit coupling between S_0 and T_1, and (iii) the final

DOI: 10.1021/acs.joc.6b02748
J. Org. Chem. 2017, 82, 2450−2461

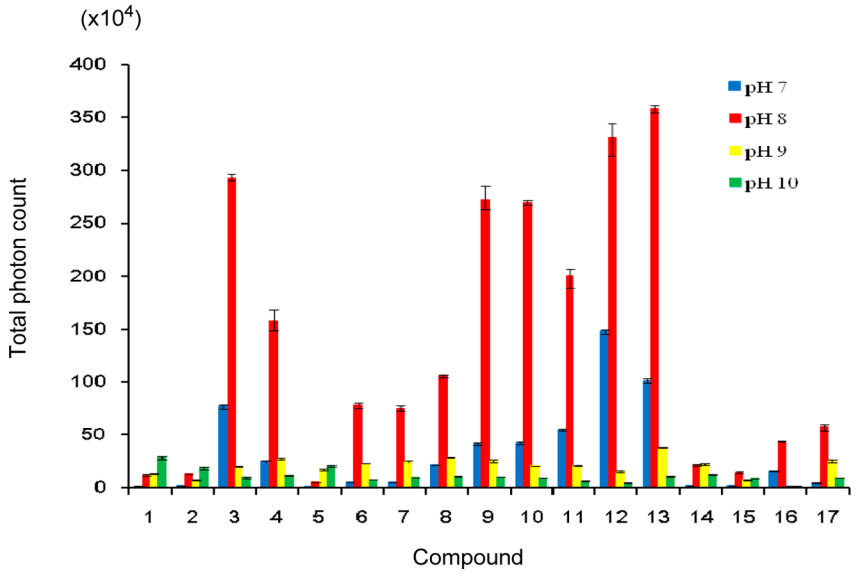

Figure 2. Effect of pH on the chemiluminescence development of compounds **1**−**17**. To a 10 nM solution of compounds **1**−**17** in dimethyl sulfoxide was added buffer solution (100 mM Tris-HCl for pH 7 and pH 8, 100 mM Gly-NaOH for pH 9 and pH 10). The CL reaction was initiated by adding 5 mM aqueous hydrogen peroxide solution to the luminometer. The CL emission was measured for 1 min, and the integral photon counts were used to evaluate the CL intensity.

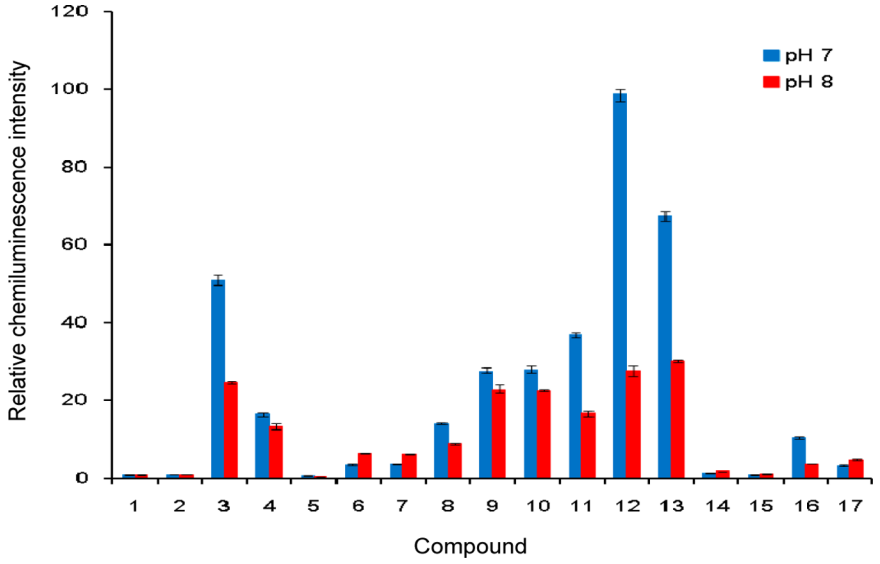

Figure 3. Relative chemiluminescence intensity of compounds **1**−**17** at pH 7 and pH 8. The concentration of compounds **1**−**17** was 10 nM. The concentration of hydrogen peroxide was 5 mM. Chemiluminescence was measured for 1 min. The CL intensity of compound **1** at each pH 7 and pH 8 was taken as 1.

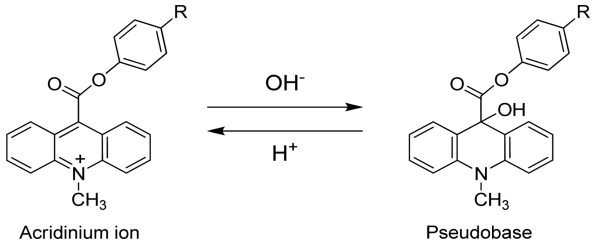

Figure 4. Equilibrium between acridinium esters and their pseudobases.

decomposition to reach acridone in T_1. The first triplet state (T_1) is electronically excited state from the viewpoint of singlet calculations based on the DFT approach, but since our interest is in the electronically ground state in triplet states, the DFT approach for the triplet ground state (T_1) was assumed to be reasonable for searching the reaction-path, rather than the TDFT approach. The polarized continuum model was also employed to reproduce the solvent effect caused by dimethyl sulfoxide (DMSO). Each energy listed in Figure 7 was confirmed by a single-point calculation for the symmetry-adapted cluster/configuration interaction (SAC-CI) method using the optimized geometry of the DFT calculation employing the same polarizable continuum model (PCM) with DMSO (Table S2 in Supporting Information).

Since the mechanism of the nucleophilic addition of hydroperoxide anion was proposed by McCapra and Nelson et al.[45,46a] and theoretically discussed by Błażejowski et al.,[56,60] the charges of acridinium ester were evaluated by natural bond

DOI: 10.1021/acs.joc.6b02748
J. Org. Chem. 2017, 82, 2450−2461

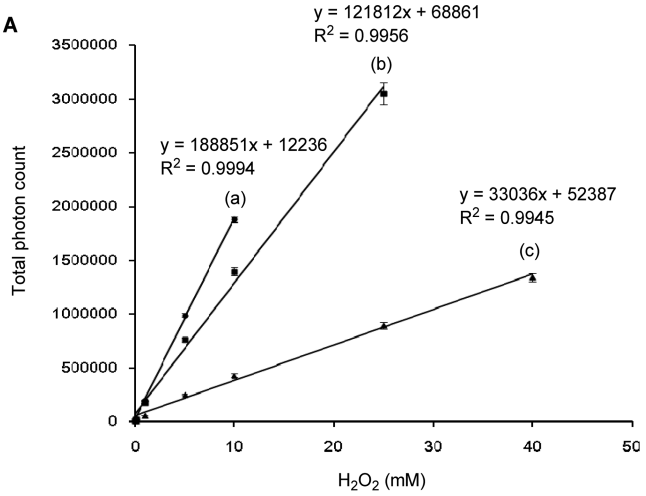

Figure 5. Standard curves of hydrogen peroxide in 100 mM Tris-HCl buffer at pH 7 and pH 8 using compounds **3**, **4**, and **13**. (A) pH 7: (a) compound **13**; (b) compound **3**; (c) compound **4**. (B) pH 8: (d) compound **13**; (e) compound **3**; (f) compound **4**. The concentration of compounds **3**, **4**, and **13** was 10 nM. Chemiluminescence was measured for 1 min.

Scheme 2. Chemiluminescence Determination of Glucose Using Compound 13 at pH 7.5

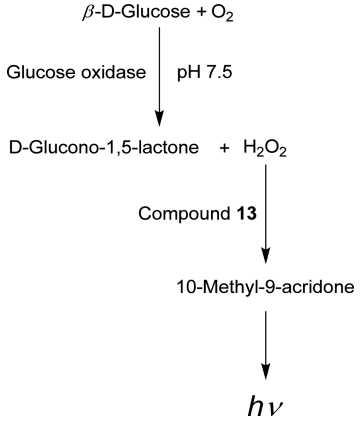

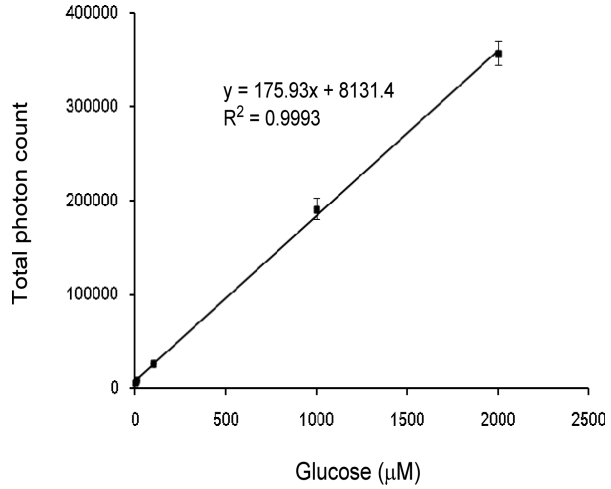

Figure 6. Standard curve of glucose at pH 7.5 using compound **13**. The concentration of compound **13** was 10 nM. Chemiluminescence was measured for 1 min.

orbital (NBO) analysis. The atomic charge at the N10 position of compound **1** shows a negative charge which is about −0.343 (−0.354) at B3-LYP (M06-2X); the hydroperoxide anion could be repulsive to the N10 side.

Figure 7A shows the energy diagram started from the dioxetanone ring-structure (**min1**) for compound **1**, which was a stable dioxetane intermediate found by Błażejowski et al.,[56,60] and then the transition state (TS) search was performed with the initial coordinate given by this **min1** structure, because the driving force for this reaction was assumed to be thermal decomposition. The TS structure appeared at **TS1** and close to the dioxetane intermediate (**min1**) as expected; the C−C bond distance in the dioxetane structure was slightly stretched, compared with **min1**. Then the reaction path (**IRC1**) on the electronic ground state (S_0) was obtained from the intrinsic reaction coordinate (IRC) analysis with the TS structure (**TS1**). The reaction path (**IRC1**) determined by the IRC analysis from **TS1** was found to be correlated to the interaction structure between the S_0 and lowest triplet (T_1) states at **int1** (Figure 8), which clearly shows the triplet state lying close to S_0. Furthermore, the S_1 state was much higher than T_1 at **int1** (Table S2(a) in Supporting Information); the vertical excitation energy of S_1 was 2.02 eV at the S_0−T_1 closest point (**int1**) by SAC-CI calculation.

As discussed in ref 62, the intersystem crossing (ISC, nonadiabatic transition in other words) mechanism was explored due to the spin−orbit coupling between S_0 and T_1 states along the reaction path **IRC1**. The potential energy curve of the T_1 state was found to be lying close to S_0 at **int1**. Thus, the nonadiabatic transition between S_0 and T_1 could happen due to the spin−orbit coupling effect at the vicinity to T_1.[63] If we assumed a nonadiabatic transition between S_0 and T_1, the molecule could be expected to hop to T_1 and be dissociated into 10-methyl-9-acridone and the fragment anion in T_1; it follows that the IRC analysis was performed again on T_1 with the **int1** structure instead of **IRC1**. The obtained reaction path (**IRC2**) is found to be correlated with the decomposition product including the triplet state of 10-methyl-9-acridone, compared to **IRC1**; the phosphorescence could be anticipated by this process. Furthermore, the transition probability due to the spin−orbit coupling was estimated by the Zhu−Nakamura formula;[63] the spin−orbit coupling elements were computed by

DOI: 10.1021/acs.joc.6b02748
J. Org. Chem. 2017, 82, 2450−2461

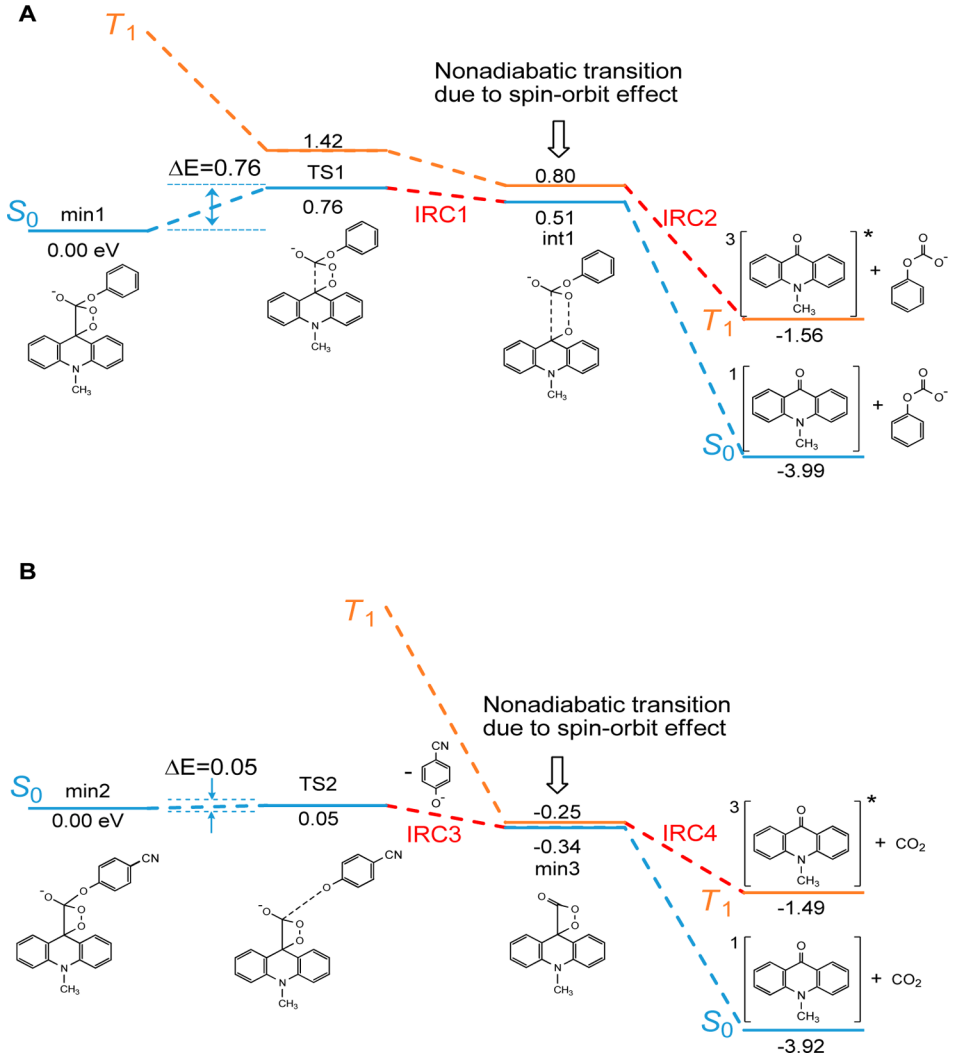

Figure 7. Energy diagram of the chemiluminescence mechanism proposed by McCapra and Nelson et al.[45,46a] (A) Compound **1**; (B) compound **3**.

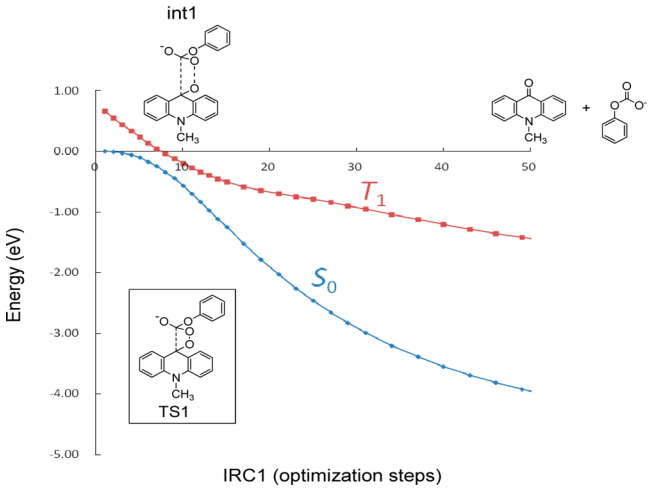

Figure 8. Intrinsic reaction coordinate determined with the initial molecular geometry of TS1 (IRC1). The employed step-width was 0.05 Bohr around the TS.

complete active space (CAS) SCF calculation by ab initio program package Molpro 2012 at cc-pVDZ basis set.[64] Using 8 CPU-cores of AMD Opteron 2382 and 8 GB ram (Tempest9D2 model, Concurrent System Ltd.) in Sophia University, it took about four months to obtain all results. However, spin−orbit coupling elements were obtained by complete active space (CAS) SCF methods at cc-pVDZ basis set. The active space was determined by (6e,4o); the electron configurations of CASSCF were totally 32758. The probability was 96% at the **int1** structure by the available excess energy proposed by Błażejowski et al.[56,60] In general, the transition probability is considered to be small for singlet−triplet transition, but there is some evidence discussed on non-adiabatic transition probability between singlet and triplet states;[65] the probabilities shown in several molecular systems are actually almost unity for intersystem crossing (ISC).

Finally, the phosphorescence might happen because the 10-methyl-9-acridone staying in T_1 could emit a photon to deactivate the excited 10-methyl-9-acridone. The phosphorescence process is discussed in a later paragraph.

We also carried out the same theoretical analysis on the compound **3** as shown in Figure 7B; the height of TS from **min2** to **TS2** was 0.05 eV, which was much smaller than the case of the compound **1** (0.76 eV). The 4-cyanophenol moiety in compound **3**, moreover, left along **IRC3** and the stable dioxetanone was produced at **min3**. The potential energy of S_0 was found to be lying close to the triplet state (T_1) at this

DOI: 10.1021/acs.joc.6b02748
J. Org. Chem. 2017, 82, 2450−2461

min3. Since the S_1 state was much higher than T_1 (see Table S2(b)), the transition by ISC to the triplet state could be crucial on the CL of compound **3**.

The potential energy of the S_0 state for compound **1** has been theoretically explored by Błażejowski,[56,60] but the exploration of electronically excited states is still necessary for the photoemission process of 10-methyl-9-acridone at the end of this reaction. It is because the electronically excited state (S_1 or T_1) of 10-methyl-9-acridone should appear as the thermal reaction product through S_0; there should be two possible paths by nonadiabatic transition to S_1 or T_1. If we are considering that the nonadiabatic transition of S_0−S_1 will happen, the energy separation (ΔE) between these states should be less than 1.0 eV. Figure 7 and Table S2 however suggest that this S_0−S_1 transition would not occur because of ΔE > 2.0 eV. On the other hand, if the nonadiabatic transition of S_0−T_1 happens, it would be because of ΔE < 1.0 eV and our estimated probability by 96% at the **int1** structure, but the phosphorescence process should be explored at the end of the reaction. The acridinium 4-cyanophenyl ester of compound **3** should be also explored in the same manner, because the reaction path on S_0 was found to be quite different from compound **1** as shown in Figure 7. As clearly seen in Table S2, the S_1 state is much higher than T_1 at each molecular conformation except for products (i.e., 10-methyl-9-acridone). Although we were not able to perform the molecular geometry optimization and IRC calculation on each conformation at SAC−CI level, the obtained triplet states reasonably agree with the trend of DFT results, especially at the geometry of the S_0−T_1 closest point at **int1** and **min3**. Assuming a photoemission from the T_1 state lying close to the S_1 state (4.15 eV at SAC-CI) at the equilibrium geometry of 10-methyl-9-acridone, the expected emission energy would be 2.43 eV at DFT (3.88 eV at SAC-CI). This emission energy from T_1 quite agrees with the experimental spectrum which features the maximum speak at 430 nm (2.88 eV). However, since the transition dipole moment between S_1 and S_0 is 1.25 a_0 at the equilibrium conformation of 10-methyl-9-acridone, the acridone would produce luminescence in the way of the final dissociation processes in **IRC2** and **IRC4**, together with vibronic allowed transitions described by the intensity borrowing mechanism (due to spin−orbit mixing) between these two excited states (S_1 and T_1) lying close to each other. The photoemission would happen in the middle of these decomposition processes.

On the other hand, a direct search for the minimum energy conical intersection (MECI) between S_0 and T_1 for compounds **1** and **3** was performed to confirm our discussion; we carried out the state-averaged CAS(6e,4o)SCF optimizations of a singlet−triplet conical intersection in vacuo.[64] The result is shown in Figure S6 (Supporting Information) for compound **1**, which is similar to the **int1** structure shown in Figure 7A. Concerning compound **3**, we also found the MECI structure at around the **min3** structure shown in Figure 7B. Thus, the thermal decomposition of acridanyl dioxetanes would happen in accord with our proposal. It is furthermore found that the solvent effect (DMSO) could not cause different paths in compounds **1** and **3**, albeit indirectly. As a result of these factors and the energy difference between **TS1** and **TS2** (barrier-height, ΔE = 0.76 and 0.05 eV), we conclude that the *p*-cyanophenolate anion is more stabilized than the phenolate anion in thermal decomposition processes, which leads to the difference between the paths for compounds **1** and **3**. Compound **3** could show a CL intensity stronger than that of compound **1**.

Furthermore, the spin−orbit coupling was also evaluated at this CASSCF level with the MECI structure for compound **1**. The potential energies of S_0 and T_1 states were shifted due to the spin−orbit coupling, as shown in Table S3 (Supporting Information); the shifted energy range is approximately 80 cm^{-1}. Since the value of atomic carbon is 43.4 cm^{-1},[66] this shifted range is obviously larger than the normal carbon atom. Probably the carbon atoms are strongly affected by the oxygen atoms. Thus, our result could reasonably support the reaction pathway through the triplet state (T_1).

CONCLUSION

Various acridinium ester derivatives were synthesized, and the chemiluminescence intensities were determined. Acridinium esters that show strong chemiluminescence intensities under neutral conditions were identified. The introduction of electron-withdrawing groups at the 4-position of the phenyl and biphenyl moiety was very effective for increasing chemiluminescence intensity; the effect would induce the polarizability not only at the specific positions in the acridine moiety but also the strong polarizability as a whole molecule. 3,4-(Dimethoxycarbonyl)phenyl 10-methyl-10λ^4-acridine-9-carboxylate trifluoromethanesulfonate salt was a useful compound for the determination of hydrogen peroxide and glucose under neutral conditions. A chemiluminescence reaction mechanism has been proposed by McCapra and Nelson et al.[45,46a] The proposed mechanism was mainly evaluated via quantum chemical calculation on density functional theory with the polarizable continuum model. The actual proposed mechanism was composed of the nucleophilic addition reaction of hydroperoxide anion, the highly strained dioxetanone ring formation, and the decomposition of the ring molecule. Natural bond orbital (NBO) charge analysis shows that the atomic charge at the C9 position in the acridine moiety was obviously more positive than at the other atoms and was quite attractive to a nucleophilic reagent such as hydroperoxide anion. The decomposition reaction would happen after the formation of the dioxetane intermediate; there was a transition state (TS) in the course of this decomposition, and it would be a rate-determining step in the whole process. Since the first triplet state (T_1) was lying close to S_0 at around the TS, nonadiabatic transition of $S_0 \rightarrow T_1$ could happen, but the photoemission of the mixed state from T_1 and S_1 states of 10-methyl-9-acridone was expected due to the intensity-borrowing mechanism at the end of the reaction. This mechanism would be consistent with the experimental result. This study should provide significant information toward the development of novel chemiluminescent acridinium esters.

EXPERIMENTAL SECTION

General Information. Melting points were uncorrected. ^1H and ^{13}C NMR spectra were recorded on 500 and 125.7 MHz spectrometers. HRMS spectra were obtained on an electrospray ionization time-of-flight (ESI-TOF) system or by fast atom bombardment (FAB).

General Procedure for the Synthesis of Compounds 1−17. To a solution of acridine-9-carbonyl chloride (0.12 g, 0.5 mmol) in dry tetrahydrofuran (10 mL) under nitrogen gas were added 4-dimethylaminopyridine (0.01 g, 0.08 mmol), the corresponding phenols (0.75 mmol), and triethylamine (2 mL). The mixture was refluxed for 2.5 h. Chloroform (150 mL) and water (100 mL) were added to the solution. The organic layer was dried with anhydrous

DOI: 10.1021/acs.joc.6b02748
J. Org. Chem. 2017, 82, 2450−2461

sodium sulfate. The filtrate was evaporated in vacuo, and the residue was purified by column chromatography (silica gel, chloroform or ethyl acetate−hexane solution) to produce the desired acridine-9-carboxylates. The acridine-9-carboxylates were N-methylated by methyl trifluoromethanesulfonate in dichloromethane and then purified by column chromatography (silica gel, chloroform−methanol) to produce the desired acridine-9-carboxylate trifluoromethanesulfonate salt.

*Phenyl 10-Methyl-10λ⁴-acridine-9-carboxylate, Trifluoromethanesulfonate Salt (**1**).* Yellow solid (0.01 g, 13%); mp 233−235 °C; ^{1}H NMR (500 MHz, acetone-d_6): δ 5.25 (s, 3H), 7.48 (m, 1H), 7.63 (m, 2H), 7.69 (m, 2H), 8.26 (m, 2H), 8.64 (m, 2H), 8.75 (d, *J* = 8.5 Hz, 2H), 9.06 (d, *J* = 9.5 Hz, 2H); ^{13}C NMR (125.7 MHz, DMSO-d_6): δ 119.9, 121.8, 122.2, 127.5, 129.8, 130.1, 139.1, 141.9, 146.8, 149.5, 163.5; HRMS ESI (*m*/*z*) calculated for $C_{21}H_{16}NO_2$ [M]$^+$ 314.1181, found 314.1177.

*p-Tolyl 10-Methyl-10λ⁴-acridine-9-carboxylate, Trifluoromethanesulfonate Salt (**2**).* Yellow solid (0.03 g, 14%); mp 232−234 °C; ^{1}H NMR (500 MHz, acetone-d_6): δ 2.43 (s, 3H), 5.24 (s, 3H), 7.43 (d, *J* = 8 Hz, 2H), 7.55 (d, *J* = 8.5 Hz, 2H), 8.25 (m, 2H), 8.64 (m, 2H), 8.72 (d, *J* = 8.5 Hz, 2H), 9.05 (d, *J* = 9.5 Hz, 2H); ^{13}C NMR (125.7 MHz, DMSO-d_6) δ 20.4, 119.9, 121.5, 122.2, 127.5, 129.7, 130.4, 136.9, 139.1, 141.9, 146.9, 147.3, 163.6; HRMS ESI (*m*/*z*) calculated for $C_{22}H_{18}NO_2$ [M]$^+$ 328.1338, found 328.1361.

*4-Cyanophenyl 10-Methyl-10λ⁴-acridine-9-carboxylate, Trifluoromethanesulfonate Salt (**3**).* Yellow solid (0.05 g, 23%); mp 278−280 °C; ^{1}H NMR (500 MHz, acetone-d_6): δ 5.25 (s, 3H), 7.98 (d, *J* = 8.5 Hz, 2H), 8.08 (d, *J* = 8.5 Hz, 2H), 8.25 (m, 2H), 8.64 (m, 2H), 8.78 (d, *J* = 8.5 Hz, 2H), 9.07 (d, *J* = 9 Hz, 2H); ^{13}C NMR (125.7 MHz, DMSO-d_6): δ 110.6, 118, 119.9, 122.3, 123.5, 127.5, 129.8, 134.6, 139.2, 141.9, 145.9, 152.5, 162.8; HRMS ESI (*m*/*z*) calculated for $C_{22}H_{15}N_2O_2$ [M]$^+$ 339.1134; found 339.1139.

*4-(Trifluoromethyl)phenyl 10-Methyl-10λ⁴-acridine-9-carboxylate, Trifluoromethanesulfonate Salt (**4**).* Yellow solid (0.03 g, 13%); mp 252−255 °C; ^{1}H NMR (500 MHz, acetone-d_6): δ 5.26 (s, 3H), 7.98 (m, 4H), 8.26 (m, 2H), 8.65 (m, 2H), 8.79 (d, *J* = 8.5 Hz, 2H), 9.07 (d, *J* = 9.5 Hz, 2H); ^{13}C NMR (125.7 MHz, DMSO-d_6): δ 119.9, 121.9, 122.3, 122.7, 123.1, 124.9, 127.1, 127.5, 128, 128.3, 129.2, 129.8, 139.2, 141.9, 146.1, 152.2, 163; HRMS ESI (*m*/*z*) calculated for $C_{22}H_{15}F_3NO_2$ [M]$^+$ 382.1055; found 382.1055.

*4-Methoxyphenyl 10-Methyl-10λ⁴-acridine-9-carboxylate, Trifluoromethanesulfonate Salt (**5**).* Yellow solid (0.04 g, 25%); mp 265−268 °C; ^{1}H NMR (500 MHz, acetone-d_6) δ 3.88 (s, 3H), 5.24 (s, 3H), 7.14 (d, *J* = 9 Hz, 2H), 7.6 (d, *J* = 9.5 Hz, 2H), 8.25 (m, 2H), 8.63 (m, 2H), 8.71 (d, *J* = 8.5 Hz, 2H), 9.05 (d, *J* = 9 Hz, 2H); ^{13}C NMR (125.7 MHz, DMSO-d_6) δ 55.7, 114.9, 119.4, 119.8, 121.9, 122.2, 122.8, 127.5, 129.7, 139.1, 141.9, 142.8, 147, 158, 163.8; HRMS ESI (*m*/*z*) calculated for $C_{22}H_{18}NO_3$ [M]$^+$ 344.1287, found 344.1294.

*4-Bromophenyl 10-Methyl-10λ⁴-acridine-9-carboxylate, Trifluoromethanesulfonate Salt (**6**).* Yellow solid (0.11 g, 63%); mp 248−250 °C; ^{1}H NMR (500 MHz, acetone-d_6) δ 5.24 (s, 3H), 7.7 (d, *J* = 9 Hz, 2H), 7.8 (d, *J* = 9 Hz, 2H), 8.24 (t, *J* = 8 Hz, 2H), 8.63 (m, 2H), 8.74 (d, *J* = 9 Hz, 2H), 9.05 (d, *J* = 9.5 Hz, 2H); ^{13}C NMR (125.7 MHz, DMSO-d_6) δ 119.9, 120, 122.3, 124.2, 127.5, 129.7, 132.9, 139.1, 141.9, 146.4, 148.6, 163.2; HRMS ESI (*m*/*z*) calculated for $C_{21}H_{15}BrNO_2$ [M]$^+$ 392.0286, found 392.0290.

*4-Iodophenyl 10-Methyl-10λ⁴-acridine-9-carboxylate, Trifluoromethanesulfonate Salt (**7**).* Yellow solid (0.05 g, 26%); mp 267−270 °C; ^{1}H NMR (500 MHz, acetone-d_6): δ 5.25 (s, 3H), 7.56 (d, *J* = 9 Hz, 2H), 7.99 (d, *J* = 8.5 Hz, 2H), 8.24 (t, *J* = 7 Hz, 2H), 8.64 (m, 2H), 8.74 (d, *J* = 9 Hz, 2H), 9.05 (d, *J* = 9.5 Hz, 2H); ^{13}C NMR (125.7 MHz, DMSO-d_6): δ 92.7, 119.9, 122.3, 124.3, 127.5, 129.7, 138.8, 139.2, 141.9, 146.4, 149.3, 163.2; HRMS ESI (*m*/*z*) calculated for $C_{21}H_{15}INO_2$ [M]$^+$ 440.0147; found 440.0140.

*4-Formylphenyl 10-Methyl-10λ⁴-acridine-9-carboxylate, Trifluoromethanesulfonate Salt (**8**).* Yellow solid (0.14 g, 57%); mp 255−258 °C; ^{1}H NMR (500 MHz, acetone-d_6): δ 5.26 (s, 3H), 7.96 (d, *J* = 8.5 Hz, 2H), 8.2 (d, *J* = 6.5 Hz, 2H), 8.26 (m, 2H), 8.65 (m, 2H), 8.79 (d, *J* = 9 Hz, 2H), 9.07 (d, *J* = 9.5 Hz, 2H), 10.15 (s, 1H); ^{13}C NMR (125.7 MHz,DMSO-d_6): δ 119.9, 122.3, 122.9, 127.5, 129.8, 131.4, 135.2, 139.2, 141.9, 146.1, 153.6, 163, 192.1; HRMS ESI (*m*/*z*) calculated for $C_{22}H_{16}NO_3$ [M]$^+$ 342.1130; found 342.1126.

*4-(Methoxycarbonyl)phenyl 10-Methyl-10λ⁴-acridine-9-carboxylate, Trifluoromethanesulfonate Salt (**9**).* Yellow solid (0.07 g, 30%); mp 250−253 °C; ^{1}H NMR (500 MHz, acetone-d_6): δ 3.96 (s, 3H), 5.25 (s, 3H), 7.88 (d, *J* = 8.5 Hz, 2H), 8.25 (m, 4H), 8.65 (m, 2H), 8.77 (d, *J* = 9 Hz, 2H), 9.07 (d, *J* = 9.5 Hz, 2H); ^{13}C NMR (125.7 MHz, DMSO-d_6): δ 52.4, 119.9, 122.3, 122.4, 127.5, 128.8, 129.8, 131.2, 139.2, 141.9, 146.2, 152.9, 163, 165.3; HRMS ESI (*m*/*z*) calculated for $C_{23}H_{18}NO_4$ [M]$^+$ 372.1236; found 372.1222.

*4-(Ethoxycarbonyl)phenyl 10-Methyl-10λ⁴-acridine-9-carboxylate, Trifluoromethanesulfonate Salt (**10**).* Yellow solid (0.01 g, 4%); mp 258−260 °C; ^{1}H NMR (500 MHz, acetone-d_6): δ 1.38 (t, *J* = 7 Hz, 3H), 4.39 (q, *J* = 7 Hz, 2H), 5.26 (s, 3H), 7.86 (d, *J* = 9 Hz, 2H), 8.25 (m, 4H), 8.65 (t, *J* = 8 Hz, 2H), 8.77 (d, *J* = 8.5 Hz, 2H), 9.07 (d, *J* = 10 Hz, 2H); ^{13}C NMR (125.7 MHz, DMSO-d_6): δ 14.1, 61.1, 119.9, 122.3, 122.4, 127.5, 129.1, 129.8, 131.1, 139.2, 141.9, 146.2, 152.8, 163, 164.8; HRMS ESI (*m*/*z*) calculated for $C_{24}H_{20}NO_4$ [M]$^+$ 386.1392; found 386.1392.

*4-Nitrophenyl 10-Methyl-10λ⁴-acridine-9-carboxylate, Trifluoromethanesulfonate Salt (**11**).* Yellow solid (0.07 g, 46%); mp 232−235 °C; ^{1}H NMR (500 MHz, acetone-d_6): δ 5.26 (s, 3H), 8.05 (d, *J* = 9 Hz, 2H), 8.26 (m, 2H), 8.5 (d, *J* = 9 Hz, 2H), 8.65 (m, 2H), 8.8 (d, *J* = 9 Hz, 2H), 9.07 (d, *J* = 9.5 Hz, 2H); ^{13}C NMR (125.7 MHz, DMSO-d_6) δ 119.9, 122.3, 123.5, 125.7, 127.5, 129.8, 139.2, 141.9, 145.8, 146.3, 153.8, 162.7. HRMS ESI (*m*/*z*) calculated for $C_{21}H_{15}N_2O_4$ [M]$^+$ 359.1032, found 359.1052.

*3,4-Dicyanophenyl 10-Methyl-10λ⁴-acridine-9-carboxylate, Trifluoromethanesulfonate Salt (**12**).* Ocherous solid (0.03 g, 12%); mp 252−254 °C; ^{1}H NMR (500 MHz, acetone-d_6): δ 5.26 (s, 3H), 8.24 (m, 2H), 8.38 (s, 2H), 8.57 (t, *J* = 1.5 Hz, 1H), 8.65 (m, 2H), 8.84 (d, *J* = 8 Hz, 2H), 9.07 (d, *J* = 9.5 Hz, 2H); ^{13}C NMR (125.7 MHz, DMSO-d_6): δ 113, 113.9, 115, 115.3, 116.7, 119.8, 122.4, 127, 127.7, 128.1, 128.3, 129.3, 129.7, 136.2, 139.2, 141.9, 145.2, 152, 162.4; HRMS FAB (*m*/*z*) calculated for $C_{23}H_{14}N_3O_2$ [M]$^+$ 364.1086; found 364.1090.

*3,4-(Dimethoxycarbonyl)phenyl 10-Methyl-10λ⁴-acridine-9-carboxylate, Trifluoromethanesulfonate Salt (**13**).* Yellow solid (0.03 g, 13%); mp 268−271 °C; ^{1}H NMR (500 MHz, acetone-d_6): δ 3.93 (s, 6H), 5.27 (s, 3H), 8.04 (m, 3H), 8.25 (m, 2H), 8.66 (m, 2H), 8.83 (d, *J* = 8.5 Hz, 2H), 9.08 (d, *J* = 9.5 Hz, 2H); ^{13}C NMR (125.7 MHz, DMSO-d_6): δ 52.9, 113, 119.8, 122.3, 125, 126.9, 127.7, 129.6, 129.8, 134.2, 139.2, 141.9, 145.9, 151.2, 162.9, 166.1, 166.5; HRMS FAB (*m*/*z*) calculated for $C_{25}H_{20}NO_6$ [M]$^+$ 430.1291; found 430.1274.

*[1,1′-Biphenyl]-4-yl 10-Methyl-10λ⁴-acridine-9-carboxylate, Trifluoromethanesulfonate Salt (**14**).* Yellow solid (0.06 g, 23%); mp 250−253 °C; ^{1}H NMR (500 MHz, DMSO-d_6): δ 4.96 (s, 3H), 7.42 (t, *J* = 7 Hz, 1H), 7.51 (t, *J* = 8 Hz, 2H), 7.76 (d, *J* = 7.5 Hz, 2H), 7.85 (d, *J* = 9 Hz, 2H), 7.91 (d, *J* = 9 Hz, 2H), 8.18 (t, *J* = 7 Hz, 2H), 8.55 (t, *J* = 8 Hz, 2H), 8.66 (d, *J* = 8.5 Hz, 2H), 8.94 (d, *J* = 9 Hz, 2H); ^{13}C NMR (125.7 MHz, DMSO-d_6): δ 119.9, 122.3, 126.9, 127.5, 127.8, 128.3, 129, 129.8, 139, 139.2, 139.5, 141.9, 146.7, 148.9, 163.5; HRMS ESI (*m*/*z*) calculated for $C_{27}H_{20}NO_2$ [M]$^+$ 390.1494; found 390.1514.

*Naphthalen-1-yl 10-Methyl-10λ⁴-acridine-9-carboxylate, Trifluoromethanesulfonate Salt (**15**).* Yellow solid (0.04 g, 50%); mp 245−248 °C; ^{1}H NMR (500 MHz, acetone-d_6): δ 5.29 (s, 3H), 7.62 (m, 2H), 7.74 (t, *J* = 8 Hz, 1H), 8.01 (d, *J* = 8.5 Hz, 1H), 8.06 (d, *J* = 8.5 Hz, 1H), 8.11 (d, *J* = 8 Hz, 2H), 8.31(m, 2H), 8.68 (m, 2H), 8.84 (d, *J* = 8 Hz, 2H), 9.1 (d, *J* = 9.5 Hz, 2H); ^{13}C NMR (125.7 MHz, DMSO-d_6): δ 118.9, 120, 122.4, 125.4, 125.7, 127.1, 127.2, 127.3, 127.6, 128.3, 129.9, 134.3, 139.2, 141.9, 144.9, 146.6, 163.4; HRMS ESI (*m*/*z*) calculated for $C_{25}H_{18}NO_2$ [M]$^+$ 364.1338; found 364.1342.

*2-Oxo-2H-chromen-4-yl 10-Methyl-10λ⁴-acridine-9-carboxylate, Trifluoromethanesulfonate Salt (**16**).* Yellow solid (0.01 g, 4%); mp 238−241 °C; ^{1}H NMR (500 MHz, acetone-d_6): δ 3.63 (s, 3H), 6.29 (s, 1H), 6.78 (m, 1H), 7.1 (m, 3H), 7.28 (d, *J* = 8.5 Hz, 1H), 7.33 (d, *J* = 9 Hz, 2H), 7.48 (m, 2H), 7.56 (m, 1H), 7.6 (m, 2H); ^{13}C NMR (125.7 MHz, DMSO-d_6): δ 91, 115.7, 116.3, 117.3, 119.6, 120.7, 121.5, 123.2, 123.9, 128, 128.9, 132.7, 138.9, 140.8, 141.8, 151.3, 153.5, 161.8, 165.6, 166.3; HRMS ESI (*m*/*z*) calculated for $C_{24}H_{16}NO_4$ [M]$^+$ 382.1079; found 382.1088.

DOI: 10.1021/acs.joc.6b02748
J. Org. Chem. 2017, 82, 2450−2461

*(3-Oxo-1,3-dihydroisobenzofuran-1,1-diyl)bis(4,1-phenylene) Bis-(10-methyl-10λ⁴-acridine-9-carboxylate), Ditrifluoromethanesulfonate Salt (**17**).* Yellow solid (0.13 g, 21%); mp 280−283 °C; ^{1}H NMR (500 MHz, DMSO-d_6): δ 4.95 (s, 6H), 7.60 (d, J = 9 Hz, 1H), 7.66 (m, 3H), 7.73 (d, J = 9 Hz, 1H), 7.77 (m, 2H), 7.84 (m, 3H), 7.96 (m, 2H), 8.03 (m, 1H), 8.13 (m, 4H), 8.26 (d, J = 9 Hz, 1H), 8.29 (d, J = 9 Hz, 1H), 8.53 (m, 3H), 8.61 (d, J = 8.5 Hz, 3H), 8.93 (d, J = 9.5 Hz, 3H); ^{13}C NMR (125.7 MHz, DMSO-d_6): δ 89.9, 119.4, 119.9, 121.4, 122, 122.3, 122.4, 122.5, 124.3, 124.7, 124.8, 126, 127.4, 128.4, 128.5, 129.1, 129.8, 130.5, 131.5, 135.5, 139.1, 139.2, 139.7, 139.8, 142, 146.4, 147.5, 149.6, 149.7, 150.1, 150.8, 150.9, 163.3, 165.2, 168.5, 168.6; HRMS ESI (m/z) calculated for $C_{50}H_{34}N_2O_6$ $[M]^{2+}$ 379.1209; found 379.1220.

General Procedure for the Synthesis of Compounds 18−26. To a solution of acridine-9-carbonyl chloride (0.12 g, 0.5 mmol) in dry tetrahydrofuran (10 mL) under nitrogen gas were added 4-dimethylaminopyridine (0.03 g, 0.25 mmol), the corresponding biphenols (0.75 mmol), and triethylamine (1.5 mL). The mixture was refluxed for 2.5 h. Chloroform (150 mL) and water (100 mL) were added to the solution. The organic layer was dried with anhydrous sodium sulfate. The filtrate was concentrated and purified by column chromatography (silica gel, chloroform) to produce the desired acridine-9-carboxylates. The acridine-9-carboxylates were N-methylated by methyl trifluoromethanesulfonate in dichloromethane and then purified by column chromatography (silica gel, chloroform−methanol) to produce the desired acridine-9-carboxylate trifluoromethanesulfonate salt.

*4′-Methyl-[1,1′-biphenyl]-4-yl 10-Methyl-10λ⁴-acridine-9-carboxylate, Trifluoromethanesulfonate Salt (**18**).* Yellow solid (0.1 g, 33%); mp 278−281 °C; ^{1}H NMR (500 MHz, DMSO-d_6): δ 2.37 (s, 3H), 4.96 (s, 3H), 7.32 (d, J = 8 Hz, 2H), 7.61 (d, J = 8.5 Hz, 1H), 7.65 (d, J = 8 Hz, 2H), 7.82 (m, 3H), 8.18 (m, 2H), 8.55 (m, 2H), 8.62 (m, 2H), 8.93 (m, 2H); ^{13}C NMR (125.7 MHz, DMSO-d_6): δ 20.6, 119.9, 122.3, 124.3, 126.7, 127.5, 128, 129.6, 129.8, 136.1, 137.2, 138.8, 139.2, 139.4, 141.9, 146.4, 146.8, 148.7, 149.3, 163.2, 163.5; HRMS ESI (m/z) calculated for $C_{28}H_{22}NO_2$ $[M]^+$ 404.1651; found 404.1678.

*4′-Ethyl-[1,1′-biphenyl]-4-yl 10-Methyl-10λ⁴-acridine-9-carboxylate, Trifluoromethanesulfonate Salt (**19**).* Yellow solid (0.02 g, 5%); mp 265−268 °C; ^{1}H NMR (500 MHz, DMSO-d_6): δ 1.22 (t, J = 7.5 Hz, 3H), 2.65 (q, J = 7.5 Hz, 2H), 4.96 (s, 3H), 7.35 (d, J = 8 Hz, 2H), 7.61 (d, J = 8.5 Hz, 1H), 7.67 (d, J = 8.5 Hz, 2H), 7.82 (d, J = 9 Hz, 1H), 7.88 (d, J = 8.5 Hz, 1H), 7.99 (d, J = 8.5 Hz, 1H), 8.15 (m, 2H), 8.53 (m, 2H), 8.62 (d, J = 8.5 Hz, 1H), 8.66 (d, J = 9 Hz, 1H), 8.93 (m, 2H); ^{13}C NMR (125.7 MHz, DMSO-d_6): δ 15.5, 27.8, 119.9, 122.3, 124.3, 126.8, 127.5, 128, 128.4, 129.8, 136.4, 138.8, 139.2, 139.5, 141.9, 143.5, 146.4, 146.8, 148.7, 149.3, 163.2, 163.5; HRMS FAB (m/z) calculated for $C_{29}H_{24}NO_2$ $[M]^+$ 418.1807; found 418.1813.

*4′-Methoxy-[1,1′-biphenyl]-4-yl 10-Methyl-10λ⁴-acridine-9-carboxylate, Trifluoromethanesulfonate Salt (**20**).* Yellow solid (0.05 g, 12%); mp 255−258 °C; ^{1}H NMR (500 MHz, DMSO-d_6): δ 3.82 (s, 3H), 4.96 (s, 3H), 7.07 (d, J = 8.5 Hz, 2H), 7.7 (d, J = 9 Hz, 2H), 7.8 (d, J = 9 Hz, 2H), 7.85 (d, J = 8.5 Hz, 2H), 8.18 (t, J = 7 Hz, 2H), 8.55 (t, J = 8 Hz, 2H), 8.65 (d, J = 8.5 Hz, 2H), 8.94 (d, J = 9.5 Hz, 2H); ^{13}C NMR (125.7 MHz, DMSO-d_6): δ 55.2, 112.9, 114.4, 119.9, 121.2, 122.2, 122.3, 127.2, 127.5, 127.7, 128, 129.8, 131.3, 139.2, 141.9, 146.8, 148.4, 159.2, 163.5; HRMS FAB (m/z) calculated for $C_{28}H_{22}NO_3$ $[M]^+$ 420.1600; found 420.1614.

*4′-Bromo-[1,1′-biphenyl]-4-yl 10-Methyl-10λ⁴-acridine-9-carboxylate, Trifluoromethanesulfonate Salt (**21**).* Yellow solid (0.08 g, 29%); mp 262−265 °C; ^{1}H NMR (500 MHz, DMSO-d_6): δ 4.96 (s, 3H), 7.7 (m, 4H), 7.86 (d, J = 9 Hz, 2H), 7.92 (d, J = 9 Hz, 2H), 8.17 (t, J = 7 Hz, 2H), 8.55 (t, J = 9.5 Hz, 2H), 8.66 (d, J = 8.5 Hz, 2H), 8.94 (d, J = 9.5 Hz, 2H); ^{13}C NMR (125.7 MHz, DMSO-d_6): δ 112.9, 119.9, 121.3, 121.4, 122.3, 122.4, 126.9, 127.5, 127.8, 128.3, 128.6, 129, 129.1, 129.8, 131.7, 131.9, 138.1, 138.2, 139.2, 141.9, 146.6, 149.2, 163.4; HRMS FAB (m/z) calculated for $C_{27}H_{19}BrNO_2$ $[M]^+$ 468.0599; found 468.0627.

*4′-(Methoxycarbonyl)-[1,1′-biphenyl]-4-yl 10-Methyl-10λ⁴-acridine-9-carboxylate, Trifluoromethanesulfonate Salt (**22**).* Yellow solid (0.09 g, 11%); mp 254−257 °C; ^{1}H NMR (500 MHz, DMSO-d_6): δ 3.9 (s, 3H), 4.96 (s, 3H), 7.9 (d, J = 8.5 Hz, 2H), 7.93 (d, J = 9 Hz, 2H), 8 (d, J = 9 Hz, 2H), 8.09 (d, J = 8.5 Hz, 2H), 8.18 (t, J = 8 Hz, 2H), 8.55 (t, J = 9.5 Hz, 2H), 8.67 (d, J = 8 Hz, 2H), 8.94 (d, J = 9.5 Hz, 2H); ^{13}C NMR (125.7 MHz, DMSO-d_6): δ 52.2, 119.9, 121.5, 122.3, 122.5, 126.8, 127.2, 127.5, 128.2, 128.7, 128.8, 129.8, 138.1, 139.2, 141.9, 143.4, 146.6, 149.6, 163.4, 166; HRMS FAB (m/z) calculated for $C_{29}H_{22}NO_4$ $[M]^+$ 448.1549; found 448.1524.

*4′-(Ethoxycarbonyl)-[1,1′-biphenyl]-4-yl 10-Methyl-10λ⁴-acridine-9-carboxylate, Trifluoromethanesulfonate Salt (**23**).* Yellow solid (0.12 g, 20%); mp 226−229 °C; ^{1}H NMR (500 MHz, DMSO-d_6): δ 1.34 (t, J = 7 Hz, 3H), 4.34 (q, J = 7 Hz, 2H), 4.96 (s, 3H), 7.9 (d, J = 9 Hz, 2H), 7.92 (d, J = 8.5 Hz, 2H), 8 (d, J = 8.5 Hz, 2H), 8.08 (d, J = 8.5 Hz, 2H), 8.18 (t, J = 8.5 Hz, 2H), 8.55 (t, J = 9 Hz, 2H), 8.67 (d, J = 8.5 Hz, 2H), 8.94 (d, J = 9 Hz, 2H); ^{13}C NMR (125.7 MHz, DMSO-d_6): δ 14.1, 60.8, 119.9, 122.3, 122.5, 127.1, 127.5, 128.7, 129.1, 129.8, 138.2, 139.2, 141.9, 143.3, 146.6, 149.6, 163.4, 165.5; HRMS FAB (m/z) calculated for $C_{30}H_{24}NO_4$ $[M]^+$ 462.1705; found 462.1685.

*4′-((Benzyloxy)carbonyl)-[1,1′-biphenyl]-4-yl 10-Methyl-10λ⁴-acridine-9-carboxylate, Trifluoromethanesulfonate Salt (**24**).* Yellow solid (0.04 g, 9%); mp 222−225 °C. ^{1}H NMR (500 MHz, DMSO-d_6): δ 4.96 (s, 3H), 5.4 (s, 2H), 7.37 (d, J = 7 Hz, 1H), 7.41 (t, J = 8 Hz, 2H), 7.49 (d, J = 7 Hz, 2H), 7.9 (d, J = 8.5 Hz, 2H), 7.93 (d, J = 8.5 Hz, 2H), 7.99 (d, J = 9 Hz, 2H), 8.12 (d, J = 8.5 Hz, 2H), 8.18 (m, 2H), 8.55 (t, J = 9 Hz, 2H), 8.67 (d, J = 8.5 Hz, 2H), 8.94 (d, J = 9 Hz, 2H); ^{13}C NMR (125.7 MHz, DMSO-d_6): δ 66.2, 119.9, 122.3, 122.6, 127.3, 127.5, 127.9, 128.1, 128.5, 128.7, 128.8, 129.8, 129.9, 136.1, 138.1, 139.2, 141.9, 143.6, 146.6, 149.6, 163.4, 165.3; HRMS FAB (m/z) calculated for $C_{35}H_{26}NO_4$ $[M]^+$ 524.1862; found 524.1861.

*4′-Nitro-[1,1′-biphenyl]-4-yl 10-Methyl-10λ⁴-acridine-9-carboxylate, Trifluoromethanesulfonate Salt (**25**).* Yellow solid (0.13 g, 45%); mp >300 °C; ^{1}H NMR (500 MHz, DMSO-d_6): δ 4.97 (s, 3H), 7.94 (d, J = 8.5 Hz, 2H), 8.05 (t, J = 8.5 Hz, 4H), 8.18 (t, J = 7.5 Hz, 2H), 8.35 (d, J = 8.5 Hz, 2H), 8.55 (m, 2H), 8.68 (d, J = 9 Hz, 2H), 8.95 (d, J = 9.5 Hz, 2H); ^{13}C NMR (125.7 MHz, DMSO-d_6): δ 119.9, 122.3, 122.7, 124.1, 127.5, 128.1, 129, 129.8, 137.1, 139.2, 141.9, 145.3, 146.5, 146.9, 150.1, 163.3; HRMS FAB (m/z) calculated for $C_{27}H_{19}N_2O_4$ $[M]^+$ 435.1345; found 435.1343.

*[1,1′:4′,1″-Terphenyl]-4-yl 10-Methyl-10λ⁴-acridine-9-carboxylate, Trifluoromethanesulfonate Salt (**26**).* Yellow solid (0.04 g, 6%); mp 279−282 °C; ^{1}H NMR (500 MHz, DMSO-d_6): δ 4.97 (s, 3H), 7.39 (t, J = 7.5 Hz, 1H), 7.49 (t, J = 8 Hz, 2H), 7.74 (d, J = 7 Hz, 2H), 7.82 (d, J = 8 Hz, 2H), 7.87 (d, J = 9 Hz, 4H), 7.98 (d, J = 8.5 Hz, 2H), 8.18 (t, J = 8.5 Hz, 2H), 8.55 (t, J = 8 Hz, 2H), 8.68 (d, J = 8.5 Hz, 2H), 8.95 (d, J = 9.5 Hz, 2H); ^{13}C NMR (125.7 MHz, DMSO-d_6): δ 112.9, 119.9, 121.3, 122.3, 122.4, 123.5, 126.5, 126.6, 126.9, 127, 127.1, 127.2, 127.4, 127.5, 127.6, 128.2, 128.9, 129, 129.1, 129.8, 137.9, 138.9, 139.2, 139.4, 139.5, 141.9, 146.7, 149, 163.5; HRMS FAB (m/z) calculated for $C_{33}H_{24}NO_2$ $[M]^+$ 466.1807; found 466.1807.

Chemiluminescence Measurement of Compounds 1−26. Chemiluminescence was measured using a Lumat LB 9507 (Berthold, Bad Wildbad, Germany) luminometer.

To 50 μL of a 10 nM solution of compounds **1**−**26** in dimethyl sulfoxide was added 100 μL of a buffer solution (100 mM Tris-HCl for pH 7 and pH 8, 100 mM Gly-NaOH for pH 9 and pH 10). After the mixture was allowed to stand for 20 s, the CL reaction was initiated by adding 100 μL of 5−100 mM aqueous hydrogen peroxide solution to the luminometer using an automatic injection system. The CL emission was measured for 1 min, and the integral photon counts were used to evaluate the CL intensity.

Standard Curves for Hydrogen Peroxide at pH 7 and pH 8 Using Compounds 3, 4, and 13. To 50 μL of a 10 nM solution of compound **3**, compound **4**, or compound **13** in dimethyl sulfoxide was added 100 μL of a buffer solution (100 mM Tris-HCl for pH 7 and pH 8). After the mixture was allowed to stand for 20 s, the CL reaction was initiated by adding 100 μL of 0−40 mM aqueous hydrogen peroxide solution to the luminometer using an automatic injection system. The CL emission was measured for 1 min, and the integral photon counts were used to evaluate the CL intensity.

DOI: 10.1021/acs.joc.6b02748
J. Org. Chem. 2017, 82, 2450−2461

Chemical Stability of Compounds 1, 3, 4, and 10−13. A 10 nM dimethyl sulfoxide solution of compounds **1**, **3**, **4**, and **10−13** was allowed to stand at 25 °C for 3 h. Then, to 50 μL of a 10 nM dimethyl sulfoxide solution of compounds **1**, **3**, **4**, and **10−13** was added 100 μL of a buffer solution (100 mM Tris-HCl, pH 7). After this mixture was allowed to stand for 20 s, the CL reaction was initiated by adding 100 μL of 5 mM aqueous hydrogen peroxide solution to the luminometer using an automatic injection system. The CL emission was measured for 1 min, and the integral photon counts were used to evaluate the CL intensity.

Standard Curves for Glucose Using Compound 13. To 250 μL of 10−2000 μM glucose in 100 mM phosphate buffer (pH 7.5) was added 250 μL of a glucose oxidase (1 U) in 100 mM phosphate buffer (pH 7.5). The reaction mixture was incubated at 37 °C for 10 min, and 100 μL of the solution mixture was initiated by adding 100 μL of 10 nM compound **13** in dimethyl sulfoxide to the luminometer using an automatic injection system. The CL emission was measured for 1 min, and the integral photon counts were used to evaluate the CL intensity.

Computational Method. Molecular structures of two compounds (**1** and **3**) and the correlated molecules were fully optimized using the density functional theory (DFT) at Becke and Lee, Yang, and Parr (B3LYP)[67,68] and Zhao and Truhlar (M06-X2)[69] levels of theory. Dunning's cc-pVDZ basis set was used.[61] Energy minima were verified by vibrational frequency analysis. To determine the energy diagram of the proposed CL reaction,[45,46a] the polarizable continuum model (PCM) was employed; the solution was dimethyl sulfoxide. The symmetry-adapted cluster/configuration interaction (SAC-CI) method was employed to confirm and search the electronically excited states by a single-point calculation with DFT-optimized geometries on PCM models. Almost all of these ab initio calculations were performed with use of the electronic structure program Gaussian 09.[70] Using 8 CPU-cores of AMD Opteron 2382 and 8 GB ram (Tempest9D2 model, Concurrent System Ltd.) in Sophia University, it took about four months to obtain all results. However, spin−orbit coupling elements were obtained by complete active space (CAS) SCF methods at cc-pVDZ basis set. The active space was determined by (6e,4o).

■ ASSOCIATED CONTENT

Supporting Information

The Supporting Information is available free of charge on the ACS Publications website at DOI: 10.1021/acs.joc.6b02748.

^{1}H and ^{13}C NMR spectra and computational data tables (PDF)

■ AUTHOR INFORMATION

Corresponding Author

*Tel: +81-92-642-6597. E-mail: nakazono@phar.kyushu-u.ac.jp.

ORCID

Manabu Nakazono: 0000-0003-2723-4264

Notes

The authors declare no competing financial interest.

■ ACKNOWLEDGMENTS

This work was performed as part of a Cooperative Research Program of the "Network Joint Research Center for Materials and Devices".

■ REFERENCES

(1) (a) Kricka, L. J. *Anal. Chem.* **1995**, *67*, 499−502. (b) Kricka, L. J. *Anal. Chem.* **1999**, *71*, 305−308. (c) Kricka, L. J. *Anal. Chim. Acta* **2003**, *500*, 279−286. (d) Kricka, L. J.; Voyta, J. C.; Bronstein, I. *Methods Enzymol.* **2000**, *305*, 370−390. (e) Park, J. Y.; Kirn, T. J.; Artis, D.; Waldman, S. A.; Kricka, L. J. *Luminescence* **2010**, *25*, 463−465. (f) Park, J. Y.; Gunpat, J.; Liu, L.; Edwards, B.; Christie, A.; Xie, X.-J.; Kricka, L. J.; Mason, R. P. *Luminescence* **2014**, *29*, 553−558.

(2) (a) Honda, K.; Imai, K.; Sekino, J. *Anal. Chem.* **1983**, *55*, 940−943. (b) Tsunoda, M.; Takezawa, K.; Imai, K. *Analyst* **2001**, *126*, 637−640. (c) Tsunoda, M.; Imai, K. *Anal. Chim. Acta* **2005**, *541*, 13−23.

(3) (a) Shimomura, O.; Wu, C.; Murai, A.; Nakamura, H. *Anal. Biochem.* **1998**, *258*, 230−235. (b) Shimomura, O.; Teranishi, K. *Luminescence* **2000**, *15*, 51−58.

(4) (a) Nakazono, M.; Hino, T.; Zaitsu, K. *J. Photochem. Photobiol., A* **2007**, *186*, 99−105. (b) Nakazono, M.; Nanbu, S.; Uesaki, A.; Kuwano, R.; Kashiwabara, M.; Zaitsu, K. *Org. Lett.* **2007**, *9*, 3583−3586. (c) Agawa, H.; Nakazono, M.; Nanbu, S.; Zaitsu, K. *Org. Lett.* **2008**, *10*, 5171−5174. (d) Nakazono, M.; Jinguji, A.; Nanbu, S.; Kuwano, R.; Zheng, Z.; Saita, K.; Oshikawa, Y.; Mikuni, Y.; Murakami, T.; Zhao, Y.; Sasaki, S.; Zaitsu, K. *Phys. Chem. Chem. Phys.* **2010**, *12*, 9783−9793.

(5) (a) Kuroda, N.; Shimoda, R.; Wada, M.; Nakashima, K. *Anal. Chim. Acta* **2000**, *403*, 131−136. (b) Wada, M.; Abe, K.; Ikeda, R.; Harada, S.; Kuroda, N.; Nakashima, K. *Talanta* **2010**, *81*, 1133−1136. (c) Elgawish, M. S.; Shimomai, C.; Kishikawa, N.; Ohyama, K.; Nakashima, K.; Kuroda, N. *Analyst* **2012**, *137*, 4802−4808.

(6) (a) Arakawa, H.; Maeda, M.; Tsuji, A. *Anal. Biochem.* **1991**, *199*, 238−242. (b) Arakawa, H.; Kanemitsu, M.; Tajima, N.; Maeda, M. *Anal. Chim. Acta* **2002**, *472*, 75−82. (c) Arakawa, H.; Masuda, K.; Tajima, N.; Maeda, M. *Luminescence* **2007**, *22*, 245−250.

(7) (a) Roda, A.; Pasini, P.; Mirasoli, M.; Michelini, E.; Guardigli, M. *Trends Biotechnol.* **2004**, *22*, 295−303. (b) Roda, A.; Di Fusco, M.; Quintavalla, A.; Guardigli, M.; Mirasoli, M.; Lombardo, M.; Trombini, C. *Anal. Chem.* **2012**, *84*, 9913−9919. (c) Di Fusco, M.; Quintavalla, A.; Trombini, C.; Lombardo, M.; Roda, A.; Guardigli, M.; Mirasoli, M. *J. Org. Chem.* **2013**, *78*, 11238−11246. (d) Roda, A.; Michelini, E.; Cevenini, L.; Calabria, D.; Calabretta, M. M.; Simoni, P. *Anal. Chem.* **2014**, *86*, 7299−7304. (e) Roda, A.; Guardigli, M.; Calabria, D.; Calabretta, M. M.; Cevenini, L.; Michelini, E. *Analyst* **2014**, *139*, 6494−6501.

(8) (a) Huang, G.; Lv, Y.; Zhang, S.; Yang, C.; Zhang, X. *Anal. Chem.* **2005**, *77*, 7356−7365. (b) Wang, W.; Lu, Y.; Zhang, S.; Wang, S.; Cao, P.; Tian, Y.; Zhang, X. *Luminescence* **2009**, *24*, 55−61. (c) Niu, W.; Kong, H.; Wang, H.; Zhang, Y.; Zhang, S.; Zhang, X. *Anal. Bioanal. Chem.* **2012**, *402*, 389−395.

(9) Teranishi, K.; Nishiguchi, T. *Anal. Biochem.* **2004**, *325*, 185−195.

(10) (a) Zhang, H.; Smanmoo, C.; Kabashima, T.; Lu, J.; Kai, M. *Angew. Chem., Int. Ed.* **2007**, *46*, 8226−8229. (b) Xin, L.; Cao, Z.; Lau, C.; Kai, M.; Lu, J. *Luminescence* **2010**, *25*, 336−342. (c) El-Mahdy, A. F. M.; Shibata, T.; Kabashima, T.; Kai, M. *Chem. Commun.* **2014**, *50*, 859−861.

(11) Zhang, Y.; Tan, C.; Fei, R.; Liu, X.; Zhou, Y.; Chen, J.; Chen, H.; Zhou, R.; Hu, Y. *Anal. Chem.* **2014**, *86*, 1115−1122.

(12) White, E. H.; Roswell, D. F. *Acc. Chem. Res.* **1970**, *3*, 54−62.

(13) Nakazono, M.; Nohta, H.; Sasamoto, K.; Ohkura, Y. *Anal. Sci.* **1992**, *8*, 779−783.

(14) Zhao, J.-Y.; Labbe, J.; Dovichi, N. J. *J. Microcolumn Sep.* **1993**, *5*, 331−339.

(15) Tsukagoshi, K.; Nakamura, T.; Nakajima, R. *Anal. Chem.* **2002**, *74*, 4109−4116.

(16) Huang, G.; Ouyang, J.; Delanghe, J. R.; Baeyens, W. R. G.; Dai, Z. *Anal. Chem.* **2004**, *76*, 2997−3004.

(17) Han, J.; Jose, J.; Mei, E.; Burgess, K. *Angew. Chem., Int. Ed.* **2007**, *46*, 1684−1687.

(18) Qi, Y.; Li, B. *Chem. - Eur. J.* **2011**, *17*, 1642−1648.

(19) Bailey, T. S.; Pluth, M. D. *J. Am. Chem. Soc.* **2013**, *135*, 16697−16704.

(20) He, Y.; Cui, H. *Chem. - Eur. J.* **2013**, *19*, 13584−13589.

(21) Griesbeck, A. G.; Diaz-Miara, Y.; Fichtler, R.; Jacobi Von Wangelin, A.; Pérez -Ruiz, R.; Sampedro, D. *Chem. - Eur. J.* **2015**, *21*, 9975−9979.

(22) Ruberto, M. A.; Grayeski, M. L. *Anal. Chem.* **1992**, *64*, 2758−2762.

(23) Sato, N. *Tetrahedron Lett.* **1996**, *37*, 8519−8522.

DOI: 10.1021/acs.joc.6b02748
J. Org. Chem. 2017, 82, 2450−2461

(24) Razavi, Z.; McCapra, F. *Luminescence* **2000**, *15*, 245−249.
(25) Renotte, R.; Sarlet, G.; Thunus, L.; Lejeune, R. *Luminescence* **2000**, *15*, 311−320.
(26) King, D. W.; Cooper, W. J.; Rusak, S. A.; Peake, B. M.; Kiddle, J. J.; O'Sullivan, D. W.; Melamed, M. L.; Morgan, C. R.; Theberge, S. M. *Anal. Chem.* **2007**, *79*, 4169−4176.
(27) Krzymiński, K.; Roshal, A. D.; Niziołek, A. *Spectrochim. Acta, Part A* **2008**, *70*, 394−402.
(28) Smith, K.; Yang, J.-J.; Li, Z.; Weeks, I.; Woodhead, J. S. *J. Photochem. Photobiol., A* **2009**, *203*, 72−79.
(29) Browne, K. A.; Deheyn, D. D.; El-Hiti, G. A.; Smith, K.; Weeks, I. *J. Am. Chem. Soc.* **2011**, *133*, 14637−14648.
(30) (a) Natrajan, A.; Sharpe, D. *Org. Biomol. Chem.* **2013**, *11*, 1026−1039. (b) Wang, S.; Natrajan, A. *RSC Adv.* **2015**, *5*, 19989−20002.
(31) Adam, W.; Baader, W. *Angew. Chem., Int. Ed. Engl.* **1984**, *23*, 166−167.
(32) Schaap, A. P.; Sandison, M. D.; Handley, R. S. *Tetrahedron Lett.* **1987**, *28*, 1159−1162.
(33) Bronstein, I.; Edwards, B.; Voyta, J. C. *J. Biolumin. Chemilumin.* **1989**, *4*, 99−111.
(34) (a) Matsumoto, M.; Suzuki, H.; Watanabe, N.; Ijuin, H. K.; Tanaka, J.; Tanaka, C. *J. Org. Chem.* **2011**, *76*, 5006−5017. (b) Tanimura, M.; Watanabe, N.; Ijuin, H. K.; Matsumoto, M. *J. Org. Chem.* **2012**, *77*, 4725−4731.
(35) Chen, Y.; Spiering, A. J. H.; Karthikeyan, S.; Peters, G. W. M.; Meijer, E. W.; Sijbesma, R. P. *Nat. Chem.* **2012**, *4*, 559−562.
(36) Kawashima, H.; Watanabe, N.; Ijuin, H. K.; Matsumoto, M. *Luminescence* **2013**, *28*, 696−704.
(37) Di Fusco, M.; Quintavalla, A.; Trombini, C.; Lombardo, M.; Roda, A.; Guardigli, M.; Mirasoli, M. *J. Org. Chem.* **2013**, *78*, 11238−11246.
(38) Zhang, N.; Francis, K. P.; Prakash, A.; Ansaldi, D. *Nat. Med.* **2013**, *19*, 500−505.
(39) (a) Weeks, I.; Beheshti, I.; McCapra, F.; Campbell, A. K.; Woodhead, J. S. *Clin. Chem.* **1983**, *29*, 1474−1479. (b) Natrajan, A.; Sharpe, D.; Costello, J.; Jiang, Q. *Anal. Biochem.* **2010**, *406*, 204−213. (c) Natrajan, A.; Sharpe, D.; Wen, D. *Org. Biomol. Chem.* **2012**, *10*, 3432−3447.
(40) Arakawa, H.; Tsuruoka, K.; Ohno, K.; Tajima, N.; Nagano, H. *Luminescence* **2014**, *29*, 374−377.
(41) Wang, W.; Ouyang, H.; Yang, S.; Wang, L.; Fu, Z. *Analyst* **2015**, *140*, 1215−1220.
(42) (a) Ciscato, L. F. M. L.; Bartoloni, F. H.; Weiss, D.; Beckert, R.; Baader, W. J. *J. Org. Chem.* **2010**, *75*, 6574−6580. (b) Maruyama, T.; Sugishita, H.; Kujira, H.; Ichikawa, M.; Hattori, Y.; Motoyoshiya, J. *Tetrahedron Lett.* **2013**, *54*, 1338−1343.
(43) Turan, I. S.; Akkaya, E. U. *Org. Lett.* **2014**, *16*, 1680−1683.
(44) (a) Schramm, S.; Weiss, D.; Navizet, I.; Roca-Sanjuán, D.; Beckert, R.; Görls, H. *ARKIVOC* **2013**, *3*, 174−188. (b) Ciscato, L. F. M. L.; Bartoloni, F. H.; Colavite, A. S.; Weiss, D.; Beckert, R.; Schramm, S. *Photochem. Photobiol. Sci.* **2014**, *13*, 32−37. (c) Schramm, S.; Ciscato, L. F. M. L.; Oesau, P.; Krieg, R.; Richter, J. F.; Navizet, I.; Roca-Sanjuan, D.; Weiss, D.; Beckert, R. *ARKIVOC* **2015**, *5*, 44−59. (d) Schramm, S.; Navizet, I.; Naumov, P.; Nath, N. K.; Berraud-Pache, R.; Oesau, P.; Weiss, D.; Beckert, R. *Eur. J. Org. Chem.* **2016**, *2016*, 678−681.
(45) McCapra, F.; Richardson, D. G.; Chang, Y. C. *Photochem. Photobiol.* **1965**, *4*, 1111−1121.
(46) (a) Nelson, N. C.; Cheikh, A. B.; Matsuda, E.; Becker, M. M. *Biochemistry* **1996**, *35*, 8429−8438. (b) Nelson, N. C.; Woodhead, J. S.; Weeks, I.; Cheikh, A. B. Eur. Pat. Appl. EP 709466A2 19960501, 1996.
(47) Wang, Z.; Yue, H.; Wang, Y.; Wang, L.; Fu, Z. *Electrophoresis* **2014**, *35*, 1000−1003.
(48) Brown, R. C.; Weeks, I.; Fisher, M.; Harbron, S.; Taylorson, C. J.; Woodhead, J. S. *Anal. Biochem.* **1998**, *259*, 142−151.
(49) Brown, R. C.; Li, Z.; Rutter, A. J.; Mu, X.; Weeks, O. H.; Smith, K.; Weeks, I. *Org. Biomol. Chem.* **2009**, *7*, 386−394.
(50) Trzybiński, D.; Skupień, M.; Krzymiński, K.; Sikorski, A.; Błażejowski, J. *Acta Crystallogr., Sect. E: Struct. Rep. Online* **2009**, *E65*, o770−o771.
(51) David-Cordonnier, M.-H.; Hildebrand, M.-P.; Baldeyrou, B.; Lansiaux, A.; Keuser, C.; Benzschawel, K.; Lemster, T.; Pindur, U. *Eur. J. Med. Chem.* **2007**, *42*, 752−771.
(52) Moteki, S. A.; Takacs, J. M. *Angew. Chem., Int. Ed.* **2008**, *47*, 894−897.
(53) Ince, M.; Gartmann, N.; Claessens, C. G.; Torres, T.; Brühwiler, D. *Org. Lett.* **2011**, *13*, 4918−4921.
(54) McCapra, F. *Acc. Chem. Res.* **1976**, *9*, 201−208.
(55) The pK_a values of phenols were obtained from a document entitled pK_a Data Compiled by R. Williams.
(56) Krzymiński, K.; Ożóg, A.; Malecha, P.; Roshal, A. D.; Wróblewska, A.; Zadykowicz, B.; Błażejowski, J. *J. Org. Chem.* **2011**, *76*, 1072−1085.
(57) Economou, A.; Panoutsou, P.; Themelis, D. G. *Anal. Chim. Acta* **2006**, *572*, 140−147.
(58) Shiang, T.-C.; Huang, C.-C.; Chang, H.-T. *Chem. Commun.* **2009**, 3437−3439.
(59) Khajvand, T.; Alijanpour, O.; Chaichi, M. J.; Vafaeezadeh, M.; Hashemi, M. M. *Anal. Bioanal. Chem.* **2015**, *407*, 6127−6136.
(60) Rak, J.; Skurski, P.; Błażejowski, J. *J. Org. Chem.* **1999**, *64*, 3002−3008.
(61) Dunning, T. H. *J. Chem. Phys.* **1989**, *90*, 1007−1023.
(62) Gundermann, K. D.; McCapra, F. *Chemiluminescence in Organic Chemistry*; Springer Verlag: Berlin, 1987.
(63) Nakamura, H. *Nonadiabatic Transition: Concepts, Basic Theories and Applications*, 2nd revised ed., World Scientific: Singapore, 2012.
(64) Werner, H.-J.; Knowles, P. J.; Knizia, G.; Manby, F. R.; Schütz, M.; Celani, P.; Györffy, W.; Kats, D.; Korona, T.; Lindh, R.; Mitrushenkov, A.; Rauhut, G.; Shamasundar, K. R.; Adler, T. B.; Amos, R. D.; Bernhardsson, A.; Berning, A.; Cooper, D. L.; Deegan, M. J. O.; Dobbyn, A. J.; Eckert, F.; Goll, E.; Hampel, C.; Hesselmann, A.; Hetzer, G.; Hrenar, T.; Jansen, G.; Köppl, C.; Liu, Y.; Lloyd, A. W.; Mata, R. A.; May, A. J.; McNicholas, S. J.; Meyer, W.; Mura, M. E.; Nicklaß, A.; O'Neill, D. P.; Palmieri, P.; Peng, D.; Pflüger, K.; Pitzer, R.; Reiher, M.; Shiozaki, T.; Stoll, H.; Stone, A. J.; Tarroni, R.; Thorsteinsson, T.; Wang, M. Version 2012.1 (see http://www.molpro.net).
(65) (a) Kobayashi, T.; Kuramochi, H.; Harada, Y.; Suzuki, Y.; Ichimura, T. *J. Phys. Chem. A* **2009**, *113*, 12088−12093. (b) Kobayashi, T.; Kuramochi, H.; Suzuki, Y.; Ichimura, T. *Phys. Chem. Chem. Phys.* **2010**, *12*, 5140−5148. (c) Kuramochi, H.; Kobayashi, T.; Suzuki, Y.; Ichimura, T. *J. Phys. Chem. B* **2010**, *114*, 8782−8789.
(66) Radzig, A. A.; Smirnov, B. M. *Springer Series in Chemical Physics, Reference data on atoms, molecules and ions*; Springer: New York, 1985.
(67) Becke, A. D. *J. Chem. Phys.* **1993**, *98*, 5648−5652.
(68) Lee, C. T.; Yang, W. T.; Parr, R. G. *Phys. Rev. B: Condens. Matter Mater. Phys.* **1988**, *37*, 785−789.
(69) Zhao, Y.; Truhlar, D. G. *Theor. Chem. Acc.* **2008**, *120*, 215−241.
(70) Frisch, M. J.; Trucks, G. W.; Schlegel, H. B.; Scuseria, G. E.; Robb, M. A.; Cheeseman, J. R.; Scalmani, G.; Barone, V.; Mennucci, B.; Petersson, G. A.; Nakatsuji, H.; Caricato, M.; Li, X.; Hratchian, H. P.; Izmaylov, A. F.; Bloino, J.; Zheng, G.; Sonnenberg, J. L.; Hada, M.; Ehara, M.; Toyota, K.; Fukuda, R.; Hasegawa, J.; Ishida, M.; Nakajima, T.; Honda, Y.; Kitao, O.; Nakai, H.; Vreven, T.; Montgomery, J. A.; Peralta, Jr., J. E.; Ogliaro, F.; Bearpark, M.; Heyd, J. J.; Brothers, E.; Kudin, K. N.; Staroverov, V. N.; Kobayashi, R.; Normand, J.; Raghavachari, K.; Rendell, A.; Burant, J. C.; Iyengar, S. S.; Tomasi, J.; Cossi, M.; Rega, N.; Millam, J. M.; Klene, M.; Knox, J. E.; Cross, J. B.; Bakken, V.; Adamo, C.; Jaramillo, J.; Gomperts, R.; Stratmann, R. E.; Yazyev, O.; Austin, A. J.; Cammi, R.; Pomelli, C.; Ochterski, J. W.; Martin, R. L.; Morokuma, K.; Zakrzewski, V. G.; Voth, G. A.; Salvador, P.; Dannenberg, J. J.; Dapprich, S.; Daniels, A. D.; Farkas, Ö.; Foresman, J. B.; Ortiz, J. V.; Cioslowski, J.; Fox, D. J. *Gaussian 09, Revision D.01*; Gaussian, Inc., Wallingford, CT, 2009.

DOI: 10.1021/acs.joc.6b02748
J. Org. Chem. 2017, 82, 2450−2461